ActaDV

Acta Dermato-Venereologica

ActaDV

Advances in dermatology and venereology

Biogeographical Landscape of the Human Face Skin Microbiome Viewed in High Definition

Michael BRANDWEIN[1,2], Garold FUKS[3], Avigail ISRAEL[2], Emmilia HODAK[4,5], Fareed SABBAH[4], Doron STEINBERG[1], Zvi BENTWICH[2], Noam SHENTAL[6] and Shiri MESHNER[2]

[1]Biofilm Research Laboratory, Institute of Dental Sciences, Faculty of Dental Medicine, The Hebrew University of Jerusalem, Jerusalem, [2]Cutaneous Microbiology Laboratory, The Skin Research Institute, The Dead Sea and Arava Science Center, Masada, [3]Department of Physics of Complex Systems, Weizmann Institute of Science, Rehovot, [4]Division of Dermatology, Rabin Medical Center, Beilinson Hospital, Petach Tikva, [5]Sackler Faculty of Medicine, Tel Aviv University, Tel Aviv and [6]Department of Mathematics and Computer Science, The Open University of Israel, Raanana, Israel

The bacterial community that colonizes the human face imparts physiochemical and physiological effects on the facial skin. These skin-microbe interactions impact dermatological, cosmetic and skincare applications due to the centrality of the human face in daily interactions. However, fine-scale characterization of the human face skin microbiome is lacking. Using 16S rRNA sequencing and 3D cartography, this study plotted and characterized the facial skin microbiome in high-definition, based on 1,649 samples from 12 individuals. Analysis yielded a number of novel insights, including that of the relative uniformity of skin microbiome composition within skin sites, site localization of certain microbes, and the interpersonal variability of the skin microbiome. The results show that high-resolution topographical mapping of the skin microbiome is a powerful tool for studying the human skin microbiome. Despite a decade of skin microbiome research, there is still much to be discovered.

SIGNIFICANCE

The health and physical appearance of the skin of the human face is important for dermatological, cosmetic and skincare purposes. The resident microorganisms that colonize the skin (the microbiome) play an important role in maintaining the physiochemical balance of the skin. This study provides the first high-resolution facial map of the human skin microbiome and provides further insights into the composition and topographic colonization patterns of the human face microbiome.

The human skin microbiome plays an important role in both health and disease. It is involved in immune training, pathogen exclusion, and its dysbiotic state can often exacerbate disease (1–3). Modern-day practices have attenuated the skin microbiome, with uncertain consequences (4–6). Products formulated to alter the skin microbiome community composition can be used for therapeutic purposes (7), highlighting its centrality in health and disease. Despite the centrality of the human face in many dermatological and cosmetic applications, its skin microbiome has not been characterized extensively.

Skin microbiome characterization presents unique opportunities compared with other anatomical sites, as its accessibility allows topographical or biogeographical profiling. Whereas other sites are characterized from a single representative sample (e.g. gut: faecal swab; oral: buccal swab; vagina: vaginal swab), the skin's large and accessible surface area necessitates understanding of local community structure for comparative studies. At its most basic level, skin sites can be classified as moist, sebaceous or dry (8, 9), whereby a known group of microorganisms occupies each habitat. More specifically, 19 different clinically relevant skin sites have been profiled using 16S rRNA (10), Internal transcribed spacer (ITS) region (11) or metagenomic (12) methodologies. Further studies examining the role of the skin microbiome in various conditions have largely chosen to sample from these sites, as their baseline characteristics are well characterized. A landmark study using 3D cartography to map the skin microbiome and metabolome went beyond these 19 sites, yet was limited to samples from 2 individuals (13).

The wealth of information regarding baseline community composition, longitudinal stability, and dysbiosis in various clinical conditions stands in contrast to the dearth of information available regarding fine-scale microbial topographical gradients between sites. The face has numerous orifices, enabling a variety of human-environment interfaces, and is important for both clinical and cosmetic purposes. This study aimed to characterize the human skin facial microbiome at high resolution, covering the entirety of one side of the human face in an effort to further our understanding of biogeographical microbial distribution on human skin. Using 3D mapping of both female and male faces, the study mapped hundreds of samples per individual to provide the most comprehensive skin microbiome map available to date. The results provide a basis for further high-resolution topographical studies and

reveal novel insights into the structure and composition of the facial skin microbiome.

MATERIALS AND METHODS

Sample collection

Twelve healthy volunteers (6 males, 6 females), aged 28–40 years, were recruited to the study. Written informed consent was obtained by volunteers according to the approved protocols and procedures received from the Helsinki Ethics Committee of the Rabin Medical Center, Petah Tikva, Israel (approval number 0153-12-RMC). Exclusion criteria for volunteers included pregnancy, the use of systemic antibiotics over the previous month, the use of any topical medication, including antibiotics, over the past month and a history of a dermatological condition. Volunteers were instructed to avoid washing, showering and application of cosmetics on the face in the 12 h preceding sampling. Samples were taken by applying D-Squame Sampling Discs (Clinical and Derm, Dallas, USA) on the entire right side of the volunteer's face and applying a uniform amount of pressure on each sampling disc using a D-Squame Pressure Instrument. Discs were removed from the volunteers' skin using sterile tweezers and stored at –80°C until DNA extraction.

DNA extraction and sequencing

DNA extraction and library preparation were carried out as described previously (14). Briefly, total DNA was extracted using the MoBio Powersoil DNA extraction kit. PCR reaction mix consisted of 10 µl Kapa HiFi HotStart Readymix (Kapa Biosystems, Wilmington, USA), 0.4 µl primer mix (10 µM of each primer), 7.6 µl Molecular Biology Water (Sigma, St Louis, MO, USA), and 2 µl template DNA. The primer mix contained 5 different primer pairs, each targeting a different region of the 16S rRNA gene. PCR conditions followed the manufacturer's instructions, with the annealing temperature set to 61°C for 15 s. DNA extraction and PCR setup were performed in a DNA/RNA UV Cleaner-Recirculator (Biosan, Riga, Latvia) located in a PCR-free facility. PCR reactions were set up in triplicate. Following PCR, triplicates were pooled and cleaned using Agencourt AMPureXP kit (Beckman Coulter, Indianapolis, USA). Barcodes and adapters were added in a second PCR reaction. Samples were pooled and cleaned using the Agencourt AMPure XP kit (Beckman Coulter). Sequencing was carried out at Hebrew University's Genomic Applications Laboratory, Ein Kerem on an Illumina MiSeq instrument, using the v2 2 x 150 kit.

Sequence analysis

Sequence reads were filtered and bacterial abundances were estimated using SMURF, an algorithm developed by the authors to combine multiple sequence reads for high-resolution microbial community profiling (15, 16). As described previously (17), raw reads were filtered if either: (*i*) Phred score was less than 30 in more than 25% of nucleotides; or (*ii*) more than 3 nucleotides had a Phred score of less than 10; or (*iii*) a read contained 1 or more ambiguous base calls (e.g. 'N'). Unique reads with low counts were discarded. Reads were matched to k-mers per amplified region. Bacterial abundances were estimated using the expectation-maximization algorithm. Taxonomy was assigned for each reconstructed amplicon based on Greengenes taxonomy (18). In cases when taxonomic information was missing or incomplete, Ribosomal Database Project (RDP) Sequence Match engine (19) was used to assign taxonomy. The 5R package used for SMURF reconstruction can be accessed at http://doi.org/10.5281/zenodo.3740525 and curated Greengenes 16S rRNA sequences and their taxonomy appear in Table S3 of Nejman et al. (16).

Statistical analysis

All statistical tests were performed in R (20) using vegan (21) and phyloseq (22) packages. Permutational Multivariate Analysis of Variance Using Distance Matrices (PERMANOVA) was used to assess significance between groups on beta-diversity indices and was carried out using the adonis command with 999 permutations. Relative abundance of highly abundant species and of Shannon diversity was topographically mapped using *ili* (23).

RESULTS

Sample description

This study analysed 1,649 samples from 12 healthy individuals totalling 275,600,825 Illumina MiSeq 300 bp reads. These were rarefied to 5,800 reads per sample and 23 samples were excluded from further analysis, as they contained fewer than 5,800 reads. Samples were grouped into categories by anatomical sites for a number of the analyses presented below. A summary of samples analysed for this study is shown in **Table I**.

Facial sites harbour different microbial communities. Initially, samples were grouped into 9 different sites; cheek, chin, eyelid, forehead, lips (perioral skin), mouth (representative sample from the oral cavity), nose, nostril and upper lip (philtrum). Community composition of all sites consisted of the same bacterial families, yet with significant differences observed in their relative abundance (**Fig. 1**A and Fig. S1[1]). *Propionibacteriaceae* dominate in forehead (55%), cheek (48%), chin (41%), nose (53%), upper lip (46%) and lip (37%). Eyelids and

---

[1]https://doi.org/10.2340/00015555-3929

Table I. Summary of samples

Sampling site	M1	M2	M3	M4	M5	M6	F1	F2	F3	F4	F5	F6	Mean
Cheek	36	44	62	62	58	53	50	74	76	61	41	66	57
Chin	16	11	8	12	18	0	14	9	8	8	13	8	10
Eyelid	2	2	2	2	3	1	2	2	2	2	2	2	2
Forehead	31	23	32	47	46	56	36	47	42	39	40	34	39
Lip	7	6	6	6	12	0	4	4	3	5	8	8	6
Mouth	1	1	1	1	1	0	1	1	1	1	1	1	1
Nose	18	20	16	18	20	8	12	13	14	17	9	14	15
Nostril	1	1	1	1	1	0	1	1	1	1	1	1	1
Upper lip	4	2	6	2	4	4	8	2	5	4	6	8	5
Total	112	108	128	149	159	118	120	151	147	134	115	134	
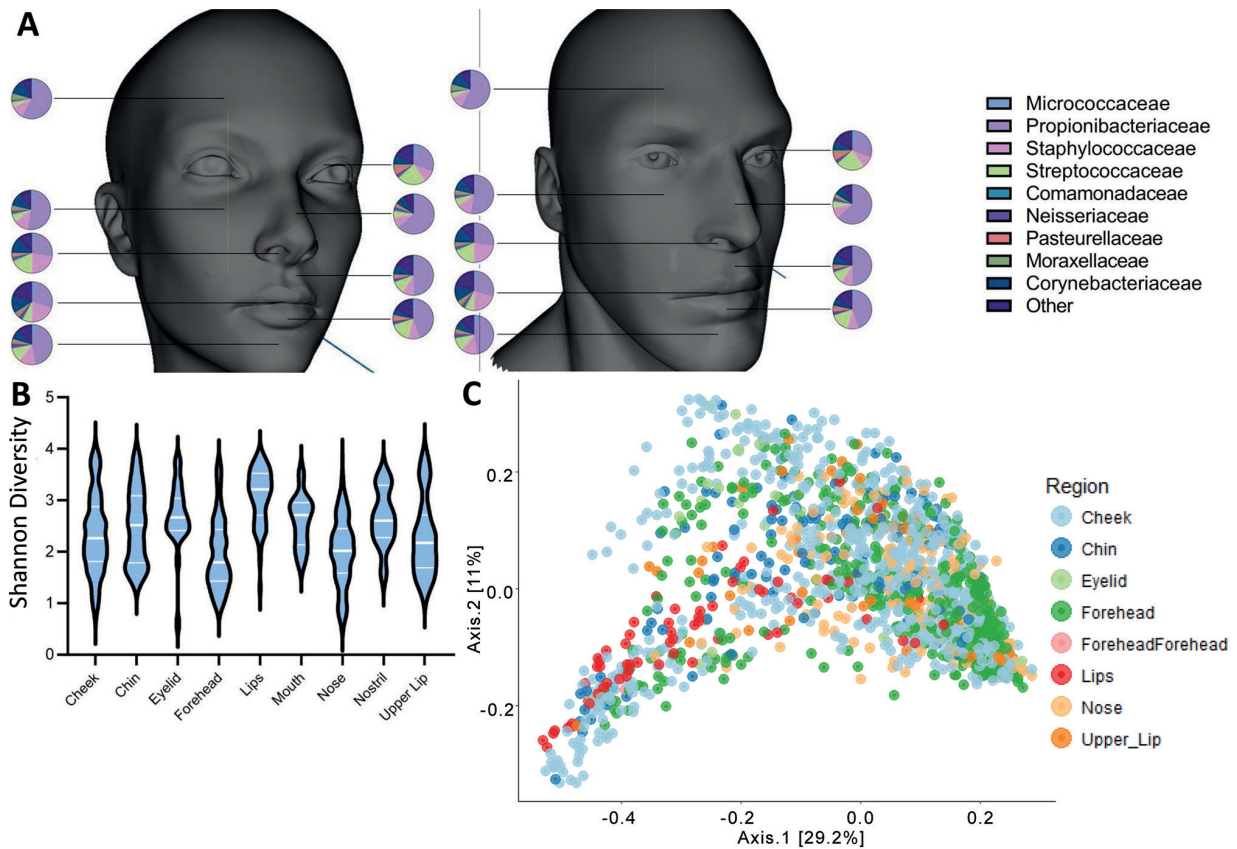
Fig. 1. Topographical diversity of the human skin facial microbiome by site. (A) Pie charts of mean community composition of 8 different facial sites, according to sex. (B) Violin plot of Shannon diversity metrics of facial sites. (C) Principal coordinate analysis of Bray-Curtis dissimilarities, coloured by facial region. Alpha diversity, beta-diversity and community composition differs from one facial region to another.

nostrils harboured higher amounts of *Streptococcaceae* (16% and 36%) than other sites and *Staphylococcaceae* were more abundant in the mouth (19%) and nostril (13%) than in other facial sites. Shannon diversity profiles across all sites were different (Fig. 1B) and clustered separately on principal coordinate analyses (PCoAs) of Bray-Curtis distance matrixes when examined on both a cohort and individual level ($p = 0.001$, Fig. 1C and Fig. S2B[1]). The lips, eyelid and mouth harboured the most diverse microbial populations and differences between these sites and other sites were most pronounced on an individual and cohort level (Figs 1B, 2A, B, and Fig. S2B[1]). Of the most abundant species in the current study, *S. mitis* localization to the lips and surrounding area was the most striking (**Fig. 2**A). Facial microbial communities were similar between sexes, with slight variations in relative abundance and Shannon diversity (Fig. S3[1]).

Interpersonal variation in the facial skin microbiome. Interpersonal variations in the composition of the skin facial microbiome were pronounced across all sites (**Fig. 3**A). Samples from individuals clustered together when examining all sites together, as well as when separated by sites (PERMANOVA: $p = 0.001$). This could also be observed when looking at Shannon diversity, which showed significant variations in community diversity between individuals across all sites (Fig. 3B), with Shannon diversity within

individuals more constant than between sites (Fig. 3B and Fig. S2B[1]). Skin microbiome similarity between individuals on certain sites was not replicated on other sites (Fig. S4[1]). Whereas *C. acnes* and *S. epidermidis* were the dominant constituents of the skin microbiome between all individuals, the next-most-abundant species differed between all individuals in the study cohort and ranged from species in the *Corynebacterium*, *Lactobacillus*, *Lactococcus*, *Micrococcus* and *Delftia* genera (Figs 2A and 3C).

DISCUSSION

This study is the first to characterize and map the skin microbiome in high-definition over a defined area of the human body. Novel insights include the relative uniformity of the skin microbiome within anatomical sites, and even between certain physiologically similar sites. This may be of clinical importance, as it was observed that carriage of *S. aureus* was not confined to the nares, yet was distributed across most of the face. The study identified which habitats were more diverse than others, which is an important observation for cosmetics and dermatology, as the stability of the microbial community may hinge on its diversity. Finally, this study recaptured previous observations of interpersonal variability, yet further honed this observation by identifying that the third-most
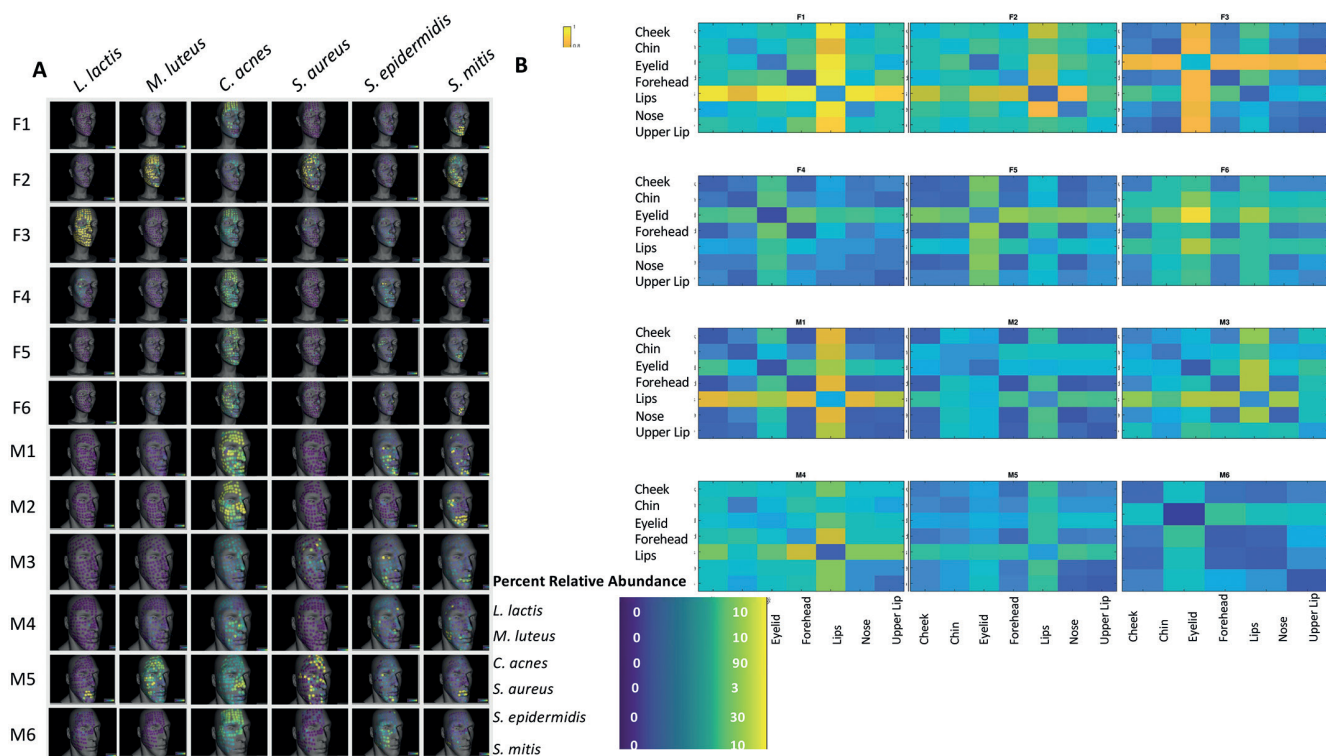
Fig. 2. High-resolution topographical diversity of the human skin facial microbiome. (A) 3D Topographically mapped relative abundance of most abundant species on each individual showing site-specificity of certain bacteria and individual-specificity of other bacteria. (B) Heatmap of mean Bray Curtis distances between sites revealing eyelids and lips as most dissimilar from other sites.

abundant species varies widely between individuals. This observation can be used for forensics or to personalize treatments and skincare applications.

Following the advancement of technology to enable skin microbiome characterization, a landmark study was published describing temporal stability, biogeographical differences and interpersonal variability of the skin microbiome (10). As this was the seminal paper on the subject, it gave rise to a plethora of studies that further refined the observations, including a higher definition look at the temporal stability of the human microbiome, first by further granulation of time (24) and subsequently using more informative methodologies (25). This granulation was not attempted with regards to topographical diversity, despite the skin's singular status as the largest epithelial surface in the human body for interaction with microorganisms (26). Skin microbiome surveys have largely used 1 of the 19 well-characterized and clinically relevant sampling sites. Other human habitats, including the oral cavity (27) and the lung (28), have been characterized to the micron level, revealing novel and intriguing community characteristics. The accessibility of the skin, coupled with its importance in a range of disciplines, including health, cosmetics, skin care and forensics necessitates a finer understanding of the topographical microbial gradients of the skin.

Previous skin microbiome surveys have used a cotton- or rayon-tipped swab soaked in NaCl-Tween solution to sample the skin microbiome. This follows the conclusion by Grice et al. (29) published over a decade ago, recom-

mending the aforementioned technique as it is gentle and involves no discomfort to the volunteer. They showed similar microbiome community profiles when using 3 separate sampling techniques surveying different depths of the skin. Notable exceptions to this methodology exist, including those specifically looking to profile the subepidermal compartments of the skin (30). The aforementioned technique did not fit the requirements of the current study, as it did not allow for side-by-side, clearly marked sampling over an entire surface without any time-lapse between sampling sites. Therefore, supported by the knowledge that skin-surface sampling methods provide similar results compared with one another, we chose to simultaneously apply D-Squame Sampling Discs over the entire sampling site to capture the entirety of the region being studied. Of note, this method most closely represents the adopted swab method, as it does not involve the use of a blade or punch-biopsy to scrape or cut deeper layers of skin.

In an effort to obtain the highest resolution microbial resolution, the Short MUltiple Regions Framework (SMURF) was applied, which amplifies several short regions along the 16S rRNA gene and then computationally combines their results to a single coherent profiling solution. SMURF solves a convex optimization problem resulting in the most likely mixture of bacteria that gave rise to the given set of reads from different regions. SMURF can be applied to any number of regions in a "mix and match" fashion, especially using any combination of common primer pairs (e.g. V1–V3, V3–V5, V4, etc.).
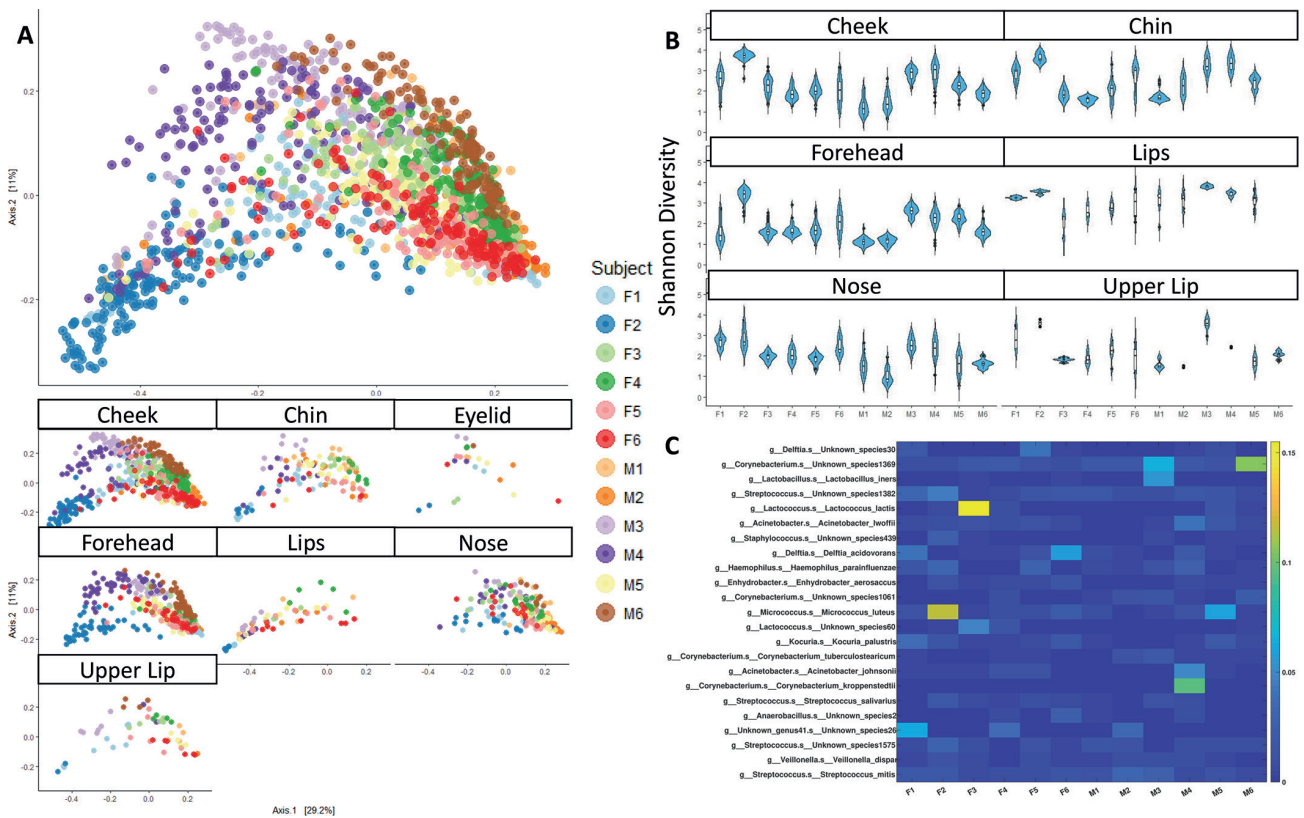
Fig. 3. Individual specific skin microbiome signatures. (A) Principal coordinate analysis of Bray-Curtis dissimilarities, coloured by individual on all sites (*upper panel*) and broken down by site (*lower panel*). (B) Shannon Diversity metrics, by site. (C) Heatmap of most abundant species (without *Cutibacterium acnes* and *Staphylococcus epidermidis*). These figures demonstrate the high variability between individuals.

The standard experimental procedure therefore remains unchanged, and the experimentalist simply selects any set of regions. The *de facto* amplicon length of SMURF is the total length across amplified regions, which significantly increases the phylogenetic resolution. For this study, 5 short regions along the 16S rRNA gene, each of length 160–240 bp, were amplified in multiplex, as described in Nejman et al. (16).

The current high-resolution study of the facial skin microbiome recaptured previously reported observations of the skin microbiome, including that of interpersonal variability and topographical or physiological influences on the skin microbiome (11, 31, 32). It added to the aforementioned observations by expanding our understanding of the fine-scale topographical changes on the facial microbiome, specifically of those on the orifices located on the face. These habitats are distinct from other skin habitats, as they bridge between other bacterial niches and that of the skin. Of additional note, cosmetics, skin care products, and other products are often applied to these areas, each of which can contribute to the composition of the skin microbiome. The localization of *S. mitis* to the area surrounding the mouth is consistent with the long-held knowledge that *S. mitis* is an oral microbe (33), and its existence on the perioral skin may be transient, as opposed to proper colonization of the area. *S. aureus*, the major skin pathobiont, is known to colonize a small

subset of the population, and it is thought that the nares serve as its reservoir in these individuals (34, 35). Our topographically mapped data indeed showed that *S. aureus* colonized a small subset of the current study cohort (*n*=2), yet colonization of the face is widespread in these individuals and is not limited to the nares or nostrils (Fig. 2A), suggesting that colonization by *S. aureus* is not limited to the nares. The observation that the third most abundant species on the face is highly individualized is intriguing, as it can potentially be used as a forensic marker or as a marker to better understand the lifestyle products and processes that contribute to the composition of the skin microbiome. This observation warrants further exploration in a larger cohort. Finally, intra-site community similarity is striking across all sites and individuals, pointing to the biogeographical uniformity of the skin microbiome when viewed in high-definition. A limitation to the current study is the small cohort (*n*=12), which was partially offset by the large number of samples taken from each individual.

In conclusion, topographical distribution of the skin microbiome reflects the complex interplay of host physiology and the exposome. Studies establishing baseline characteristics of different skin sites have been instrumental for future studies of the skin microbiome in both health and disease, yet their scale was limited. We characterized the high-resolution biogeographical distribution of the facial skin microbiome and uncovered a number of novel observa-

tions, including the localization of *S. mitis* to the perioral skin, the widespread colonization of *S. aureus* on facial skin of *S. aureus* carriers, the high diversity of the eyelids and lips, and the strong interpersonal differences of the skin microbiome in the current cohort. Importantly, the within-site distribution of bacteria on the human face is observed across all sites and members of our cohort, suggesting that minute changes in skin structure and physiology do not affect the composition of the microbiome. This information can be used in a number of fields, and it is our hope that this methodology will be repeated on other anatomical sites, leading to a complete high-resolution map of the skin microbiome.

ACKNOWLEDGEMENTS

REFERENCES

1. Brandwein M, Fuks G, Israel A, Nejman D, Straussman R, Hodak E, et al. Identification of a unique Staphylococcus aureus ribosomal signature in severe atopic dermatitis. Br J Dermatol 2018; 179: 1222–1224.
2. Gimblet C, Meisel JS, Loesche MA, Cole SD, Horwinski J, Novais FO, et al. Cutaneous leishmaniasis induces a transmissible dysbiotic skin microbiota that promotes skin inflammation. Cell Host Microbe 2017; 22: 13–24.e14.
3. Nakamura Y, Oscherwitz J, Cease KB, Chan SM, Muñoz-Planillo R, Hasegawa M, et al. Staphylococcus δ-toxin induces allergic skin disease by activating mast cells. Nature 2013; 503: 397–401.
4. Brandwein M, Katz I, Katz A, Kohen R. Beyond the gut: skin microbiome compositional changes are associated with BMI. Hum Microb J 2019; 13: 100063.
5. Two AM, Nakatsuji T, Kotol PF, Arvanitidou E, Du-Thumm L, Hata TR, et al. The cutaneous microbiome and aspects of skin antimicrobial defense system resist acute treatment with topical skin cleansers. J Invest Dermatol 2016; 136: 1950–1954.
6. SanMiguel AJ, Meisel JS, Horwinski J, Zheng Q, Bradley CW, Grice EA. Antiseptic agents elicit short-term, personalized, and body site–specific shifts in resident skin bacterial communities. J Invest Dermatol 2018; 138: 2234–2243.
7. Totte JE, van Doorn MB, Pasmans SG. Successful treatment of chronic Staphylococcus aureus-related dermatoses with the topical endolysin Staphefekt SA. 100: a report of 3 cases. Case Rep Dermatol 2017; 9: 19–25.
8. Byrd AL, Belkaid Y, Segre JA. The human skin microbiome. Nat Rev Microbiol 2018; 16: 143.
9. Grice EA, Segre JA. The skin microbiome. Nat Rev Microbiol 2011; 9: 244–253.
10. Grice EA, Kong HH, Conlan S, Deming CB, Davis J, Young AC, et al. Topographical and temporal diversity of the human skin microbiome. Science 2009; 324: 1190–1192.
11. Findley K, Oh J, Yang J, Conlan S, Deming C, Meyer JA, et al. Topographic diversity of fungal and bacterial communities in human skin. Nature 2013; 498: 367–370.
12. Oh J, Byrd AL, Deming C, Conlan S, Kong HH, Segre JA, et al. Biogeography and individuality shape function in the human skin

13. Bouslimani A, Porto C, Rath CM, Wang M, Guo Y, Gonzalez A, et al. Molecular cartography of the human skin surface in 3D. Proc Natl Acad Sci U S A 2015; 112: E2120–E2129.
14. Brandwein M, Fuks G, Israel A, Al-Ashhab A, Nejman D, Straussman R, et al. Temporal stability of the healthy human skin microbiome following dead sea climatotherapy. Acta Derm Venereol 2018; 98: 256–261.
15. Fuks G, Elgart M, Amir A, Zeisel A, Turnbaugh PJ, Soen Y, et al. Combining 16S rRNA gene variable regions enables high-resolution microbial community profiling. Microbiome 2018; 6: 17.
16. Nejman D, Livyatan I, Fuks G, Gavert N, Zwang Y, Geller LT, et al. The human tumor microbiome is composed of tumor type-specific intracellular bacteria. Science 2020; 368: 973–980.
17. Brandwein M, Fuks G, Israel A, Sabbah F, Hodak E, Szitenberg A, et al. Skin microbiome compositional changes in atopic dermatitis patients accompany dead sea climatotherapy. Photochem Photobiol 2019; 95: 1446–1453.
18. DeSantis TZ, Hugenholtz P, Larsen N, Rojas M, Brodie EL, Keller K, et al. Greengenes, a chimera-checked 16S rRNA gene database and workbench compatible with ARB. Appl Environ Microbiol 2006; 72: 5069–5072.
19. Cole JR, Chai B, Farris RJ, Wang Q, Kulam S, McGarrell DM, et al. The Ribosomal Database Project (RDP-II): sequences and tools for high-throughput rRNA analysis. Nucleic Acids Res 2005; 33: D294–D296.
20. TEAM RC. R: a language and environment for statistical computing. R Foundation for Statistical Computing, Vienna, Austria. ISBN 3–900051–07–0. [Accessed December 18, 2019] Available from: http://www.R-project org, 2010.
21. Oksanen J, Kindt R, Legendre P, O'Hara B, Stevens MHH, Oksanen MJ, et al. The vegan package. Community Ecology Package 2007; 10: 631–637.
22. McMurdie PJ, Holmes S. phyloseq: an R package for reproducible interactive analysis and graphics of microbiome census data. PloS One 2013; 8: e61217.
23. Protsyuk I, Melnik AV, Nothias L-F, Rappez L, Phapale P, Aksenov AA, et al. 3D molecular cartography using LC–MS facilitated by Optimus and'ili software. Nat Protoc 2018; 13: 134.
24. Caporaso JG, Lauber CL, Costello EK, Berg-Lyons D, Gonzalez A, Stombaugh J, et al. Moving pictures of the human microbiome. Genome Biol 2011; 12: 1–8.
25. Oh J, Byrd AL, Park M, Kong HH, Segre JA, Program NCS. Temporal stability of the human skin microbiome. Cell 2016; 165: 854–866.
26. Gallo RL. Human skin is the largest epithelial surface for interaction with microbes. J Invest Dermatol 2017; 137: 1213–1214.
27. Welch JLM, Ramírez-Puebla ST, Borisy GG. Oral microbiome geography: micron-scale habitat and niche. Cell Host Microbe 2020; 28: 160–168.
28. Garg N, Wang M, Hyde E, da Silva RR, Melnik AV, Protsyuk I, et al. Three-dimensional microbiome and metabolome cartography of a diseased human lung. Cell Host Microbe 2017; 22: 705–716.e4.
29. Grice EA, Kong HH, Renaud G, Young AC, Bouffard GG, Blakesley RW, et al. A diversity profile of the human skin microbiota. Genome Res 2008; 18: 1043–1050.
30. Nakatsuji T, Chiang H-I, Jiang SB, Nagarajan H, Zengler K, Gallo RL. The microbiome extends to subepidermal compartments of normal skin. Nat Commun 2013; 4: 1431.
31. Flores GE, Caporaso JG, Henley JB, Rideout JR, Domogala D, Chase J, et al. Temporal variability is a personalized feature of the human microbiome. Genome Biol 2014; 15: 531.
32. Brandwein M, Horev A, Bogen B, Fuks G, Israel A, Shalom G, et al. The role of sweat in the composition of skin microbiome: lessons learned from patients with congenital insensitivity to pain with anhidrosis. J Eur Acad Dermatol Venereol 2020; 34: e183–e186.
33. Engen SA, Rørvik GH, Schreurs O, Blix IJ, Schenck K. The oral commensal Streptococcus mitis activates the aryl hydrocarbon receptor in human oral epithelial cells. Int J Oral Sci 2017; 9: 145–150.
34. Mergenhagen KA, Starr KE, Wattengel BA, Lesse AJ, Sumon Z, Sellick JA. Determining the utility of methicillin-resistant Staphylococcus aureus nares screening in antimicrobial stewardship. Clin Infect Dis 2020; 71: 1142–1148.
35. Oh J, Conlan S, Polley EC, Segre JA, Kong HH. Shifts in human skin and nares microbiota of healthy children and adults. Genome Med 2012; 4: 77.

metagenome. Nature 2014; 514: 59–64.